

Supplement of The Cryosphere, 13, 3337–3352, 2019
<https://doi.org/10.5194/tc-13-3337-2019-supplement>
© Author(s) 2019. This work is distributed under
the Creative Commons Attribution 4.0 License.



Supplement of

Changing characteristics of runoff and freshwater export from watersheds draining northern Alaska

Michael A. Rawlins et al.

Correspondence to: Michael A. Rawlins (rawlins@geo.umass.edu)

The copyright of individual parts of the supplement might differ from the CC BY 4.0 License.

References

- Brodzick, M. J. and Knowles, K.: EASE-Grid: A Versatile Set of Equal-Area Projections and Grids, in M. Goodchild (Ed.) *Discrete Global Grids*. Santa Barbara, CA, USA: National Center for Geographic Information and Analysis., 2002. 11
- Food and Agriculture Organization/UNESCO: *Digital Soil Map of the World and Derived Properties*, version 3.5, November, 1995. Original scale 1:5,000,000, UNESCO, Paris, France, 1995. 2
- Hugelius, G., Strauss, J., Zubrzycki, S., Harden, J. W., Schuur, E., Ping, C.-L., Schirmer, L., Grosse, G., Michaelson, G. J., Koven, C. D., and O'Donnell, J.: Estimated stocks of circumpolar permafrost carbon with quantified uncertainty ranges and identified data gaps, *Biogeosciences*, 11, 6573–6593, <https://doi.org/10.5194/bg-11-6573-2014>, 2014. 2
- Nicolsky, D. J., Romanovsky, V., Panda, S., Marchenko, S., and Muskett, R.: Applicability of the ecosystem type approach to model permafrost dynamics across the Alaska North Slope, *J. Geophys. Res.-Earth*, 122, 50–75, <https://doi.org/10.1002/2016JF003852>, 2017. 3
- Stuefer, S., Kane, D. L., and Liston, G. E.: In situ snow water equivalent observations in the US Arctic, *Hydrol. Res.*, 44, 21–34, <https://doi.org/10.2166/nh.2012.177>, 2013. 5

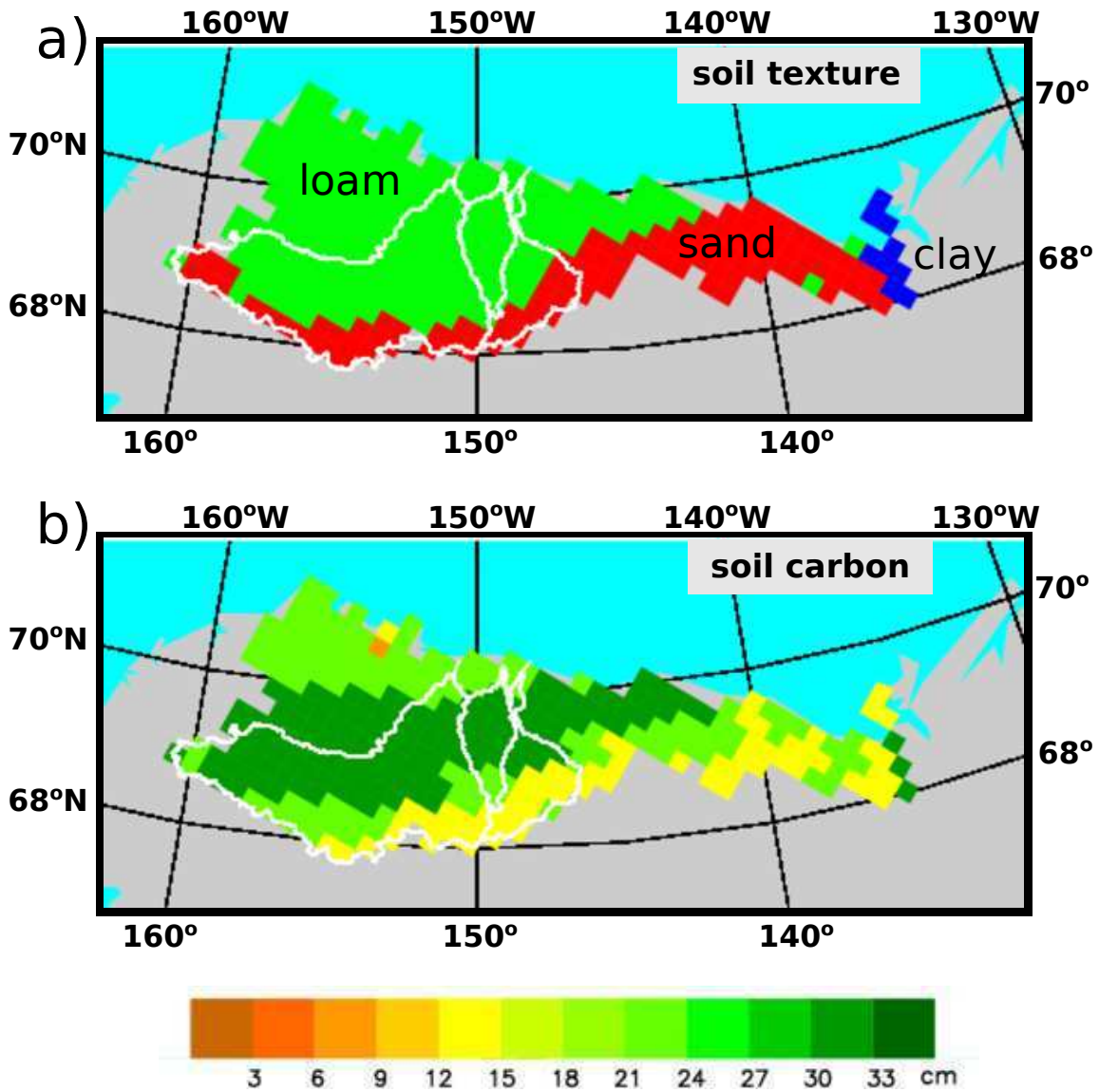


Figure S1: a) Soil texture classes and b) thickness of surface soil carbon layer used in model parameterizations. Soil textures are drawn from the UNESCO Food and Agriculture Organization’s Digital Soil Map of the World (Food and Agriculture Organization/UNESCO). Soil carbon is taken from the Northern Circumpolar Soil Carbon Database (NCSCD) (Hugelius et al., 2014). Soil carbon thickness derived from the NCSCD data and used in the PWBM includes all soil layers for which some amount of carbon is present. Primarily mineral soil exists downward over the remainder of the soil column.

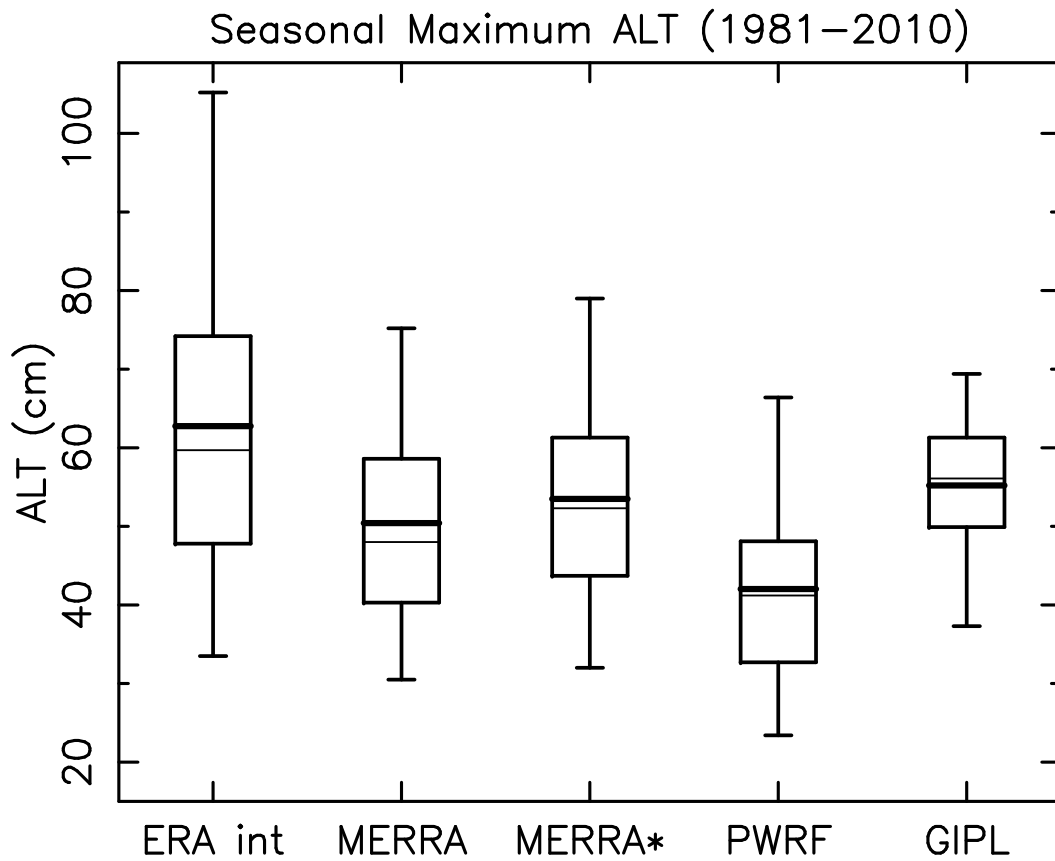


Figure S2: a) Seasonal maximum ALT (cm) as an average over the period 1981–2010 from PWBM simulations and the GIPL model. Boxplots represent the 217 (of 312) PWBM domain grid cells for which GIPL ALT data are available. Boxplots were drawn from PWBM simulation using climate forcings from ERA interim, MERRA, MERRA with precipitation adjustment (MERRA*), and Polar WRF. Heavy line in each box is the distribution mean. Thin line is the distribution median. Boxes bracket the 25th and 75th percentiles. Whiskers show the 5th and 95th percentiles. From PWBM soil temperatures the seasonal maximum ALT is calculated as the depth to which the 0 °C penetrates each summer. Nicolsky et al. (2017) provide details on the GIPL ALT.

Seasonal Maximum ALT

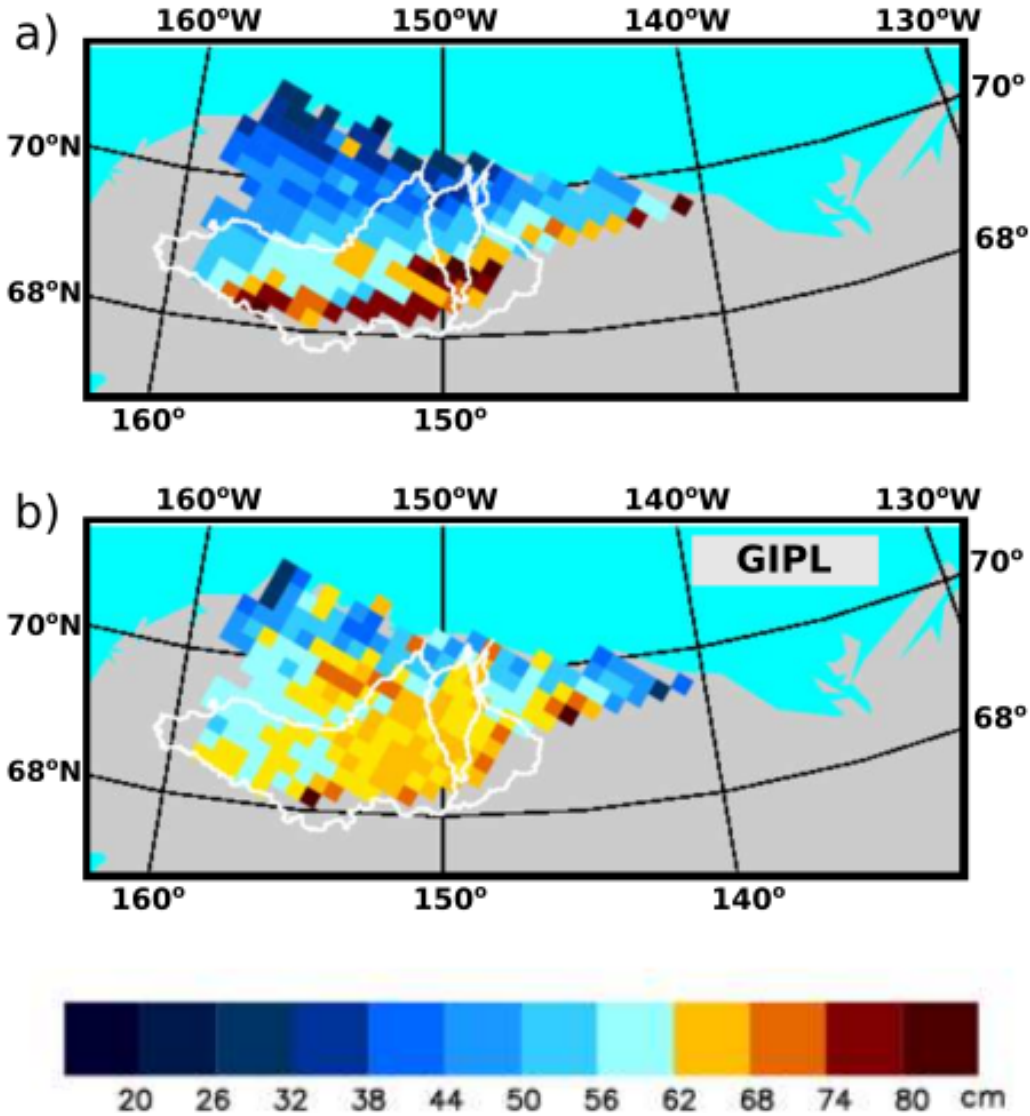


Figure S3: a) Seasonal maximum ALT (cm) as an average over the period 1981-2010 from a) PWBM with MERRA* forcing and b) GIPL.

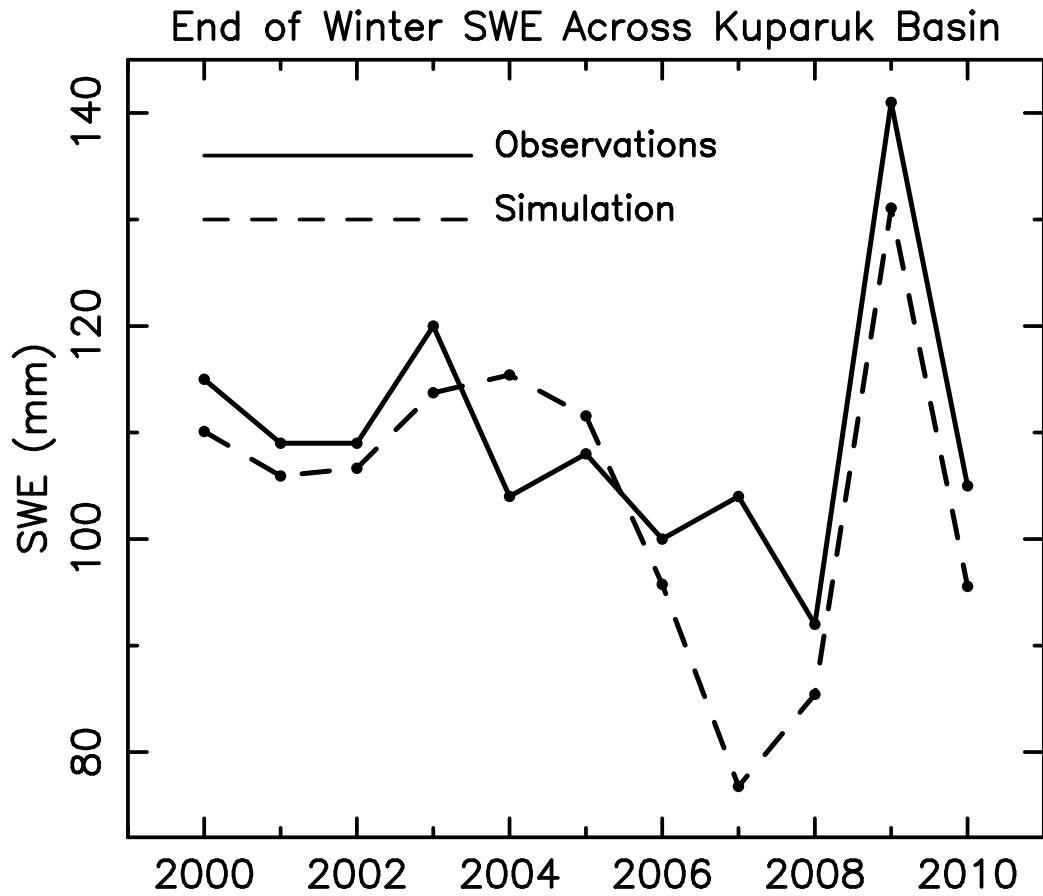


Figure S4: Observed and model simulated end of winter snow water equivalent (SWE, mm) averaged over the Kuparuk River basin 2000–2010. Observed values represent the average of measurements as described by Stuefer et al. (2013). Simulated end of season SWE is calculated as the average between 24 April and 7 May each year.

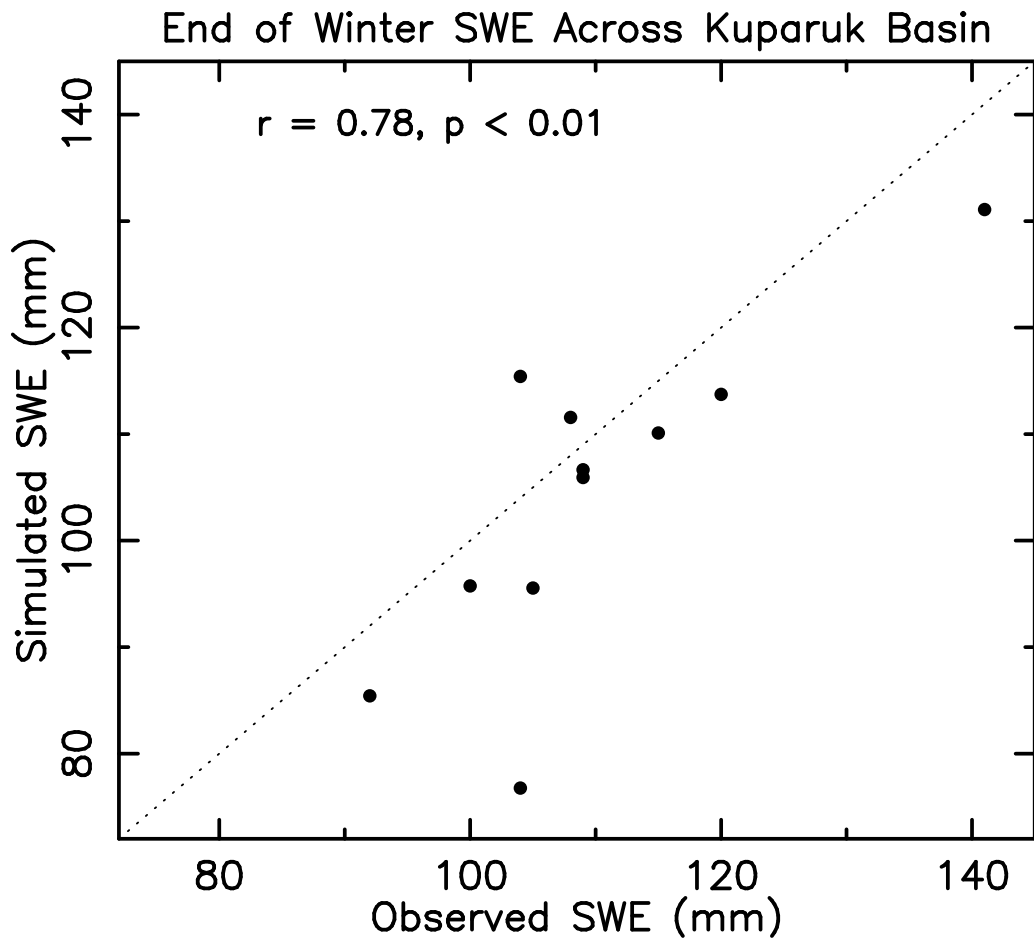


Figure S5: Observed and model simulated end of winter SWE (mm) for the Kuparuk Basin 2000–2010.

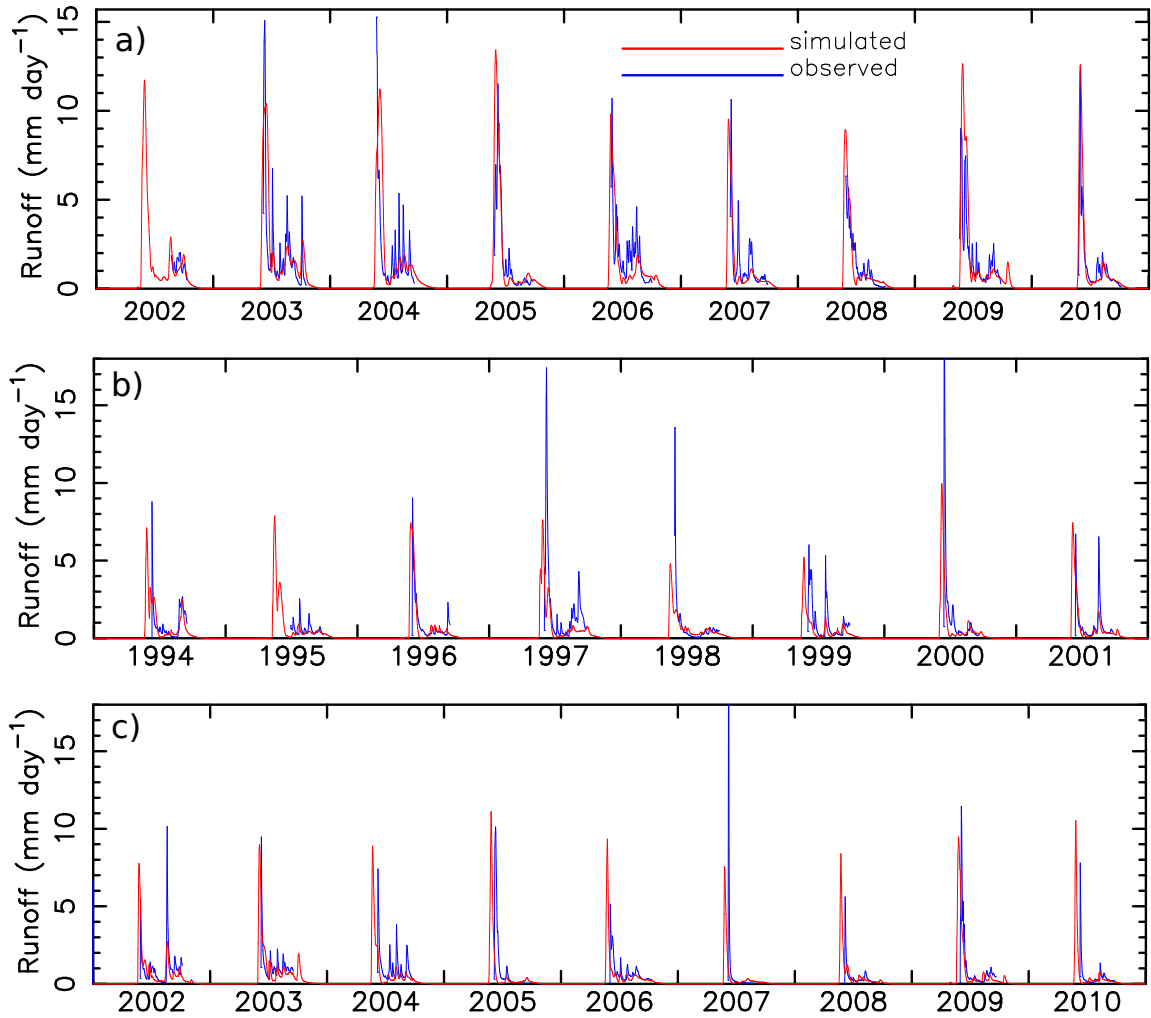


Figure S6: Simulated vs observed daily R (mm yr^{-1}) for the (a) Colville River at Umiat, AK and (b and c) Kuparuk River at Deadhorse. Simulated R is calculated from the routed river discharge (Q) at the model grid cell where Umiat and Deadhorse are located, respectively.

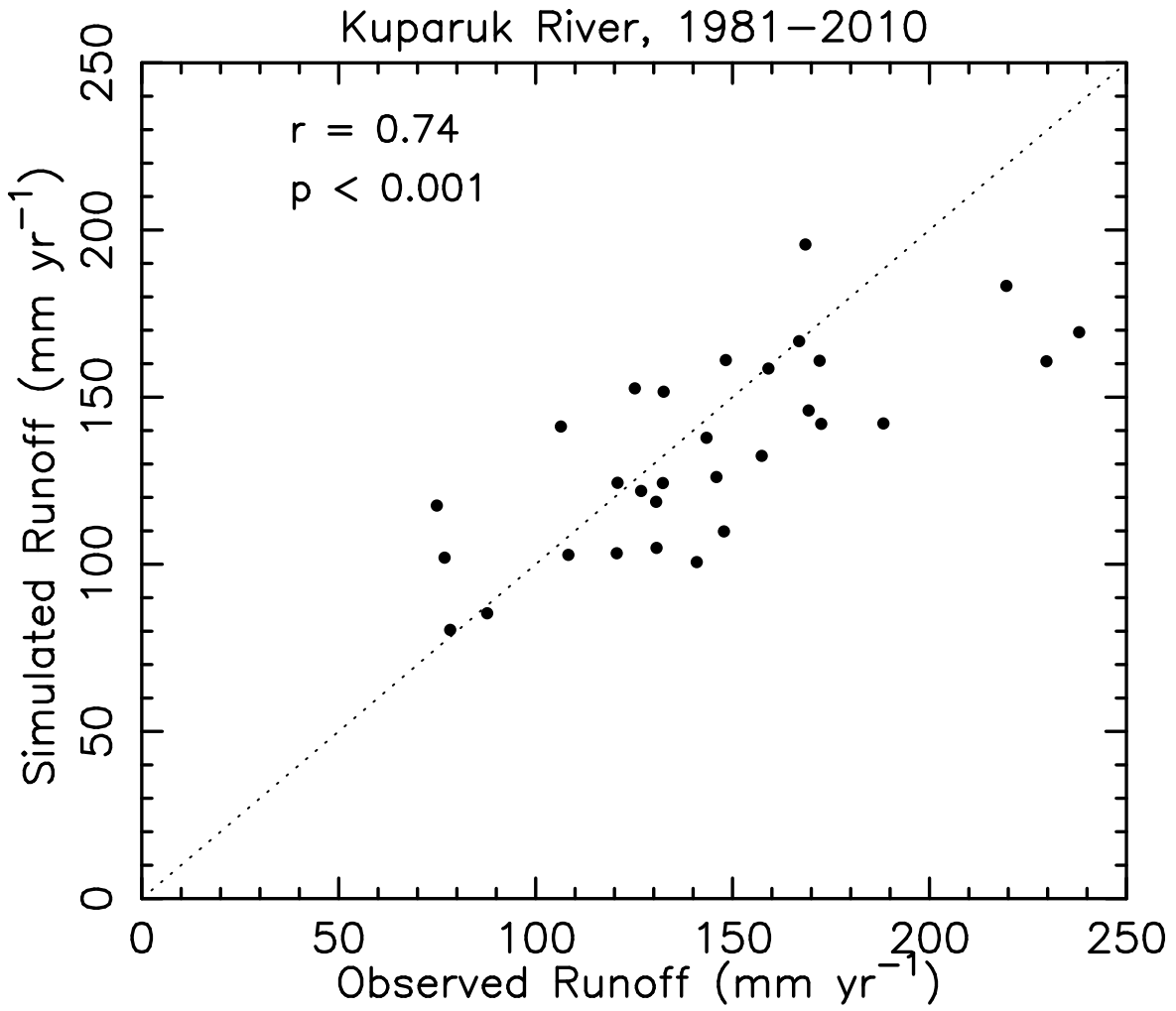


Figure S7: Simulated vs observed annual total R (mm yr^{-1}) for the Kuparuk basin. Correlation coefficient (LLS) is $r = 0.73$ ($p < 0.001$).

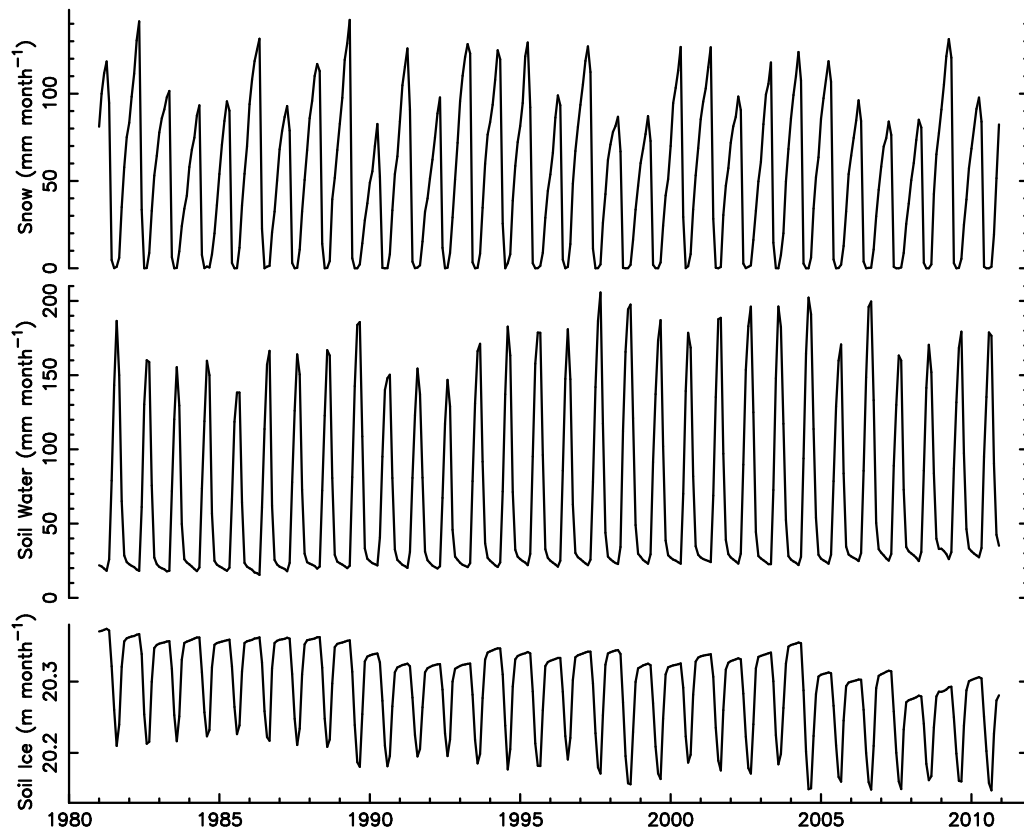


Figure S8: Monthly water storage for snow (solid and liquid portions, mm month⁻¹), soil water (mm month⁻¹), and soil ice (m month⁻¹) as an average across the North Slope drainage basin. Amounts are totaled over the full 60 m model soil column.

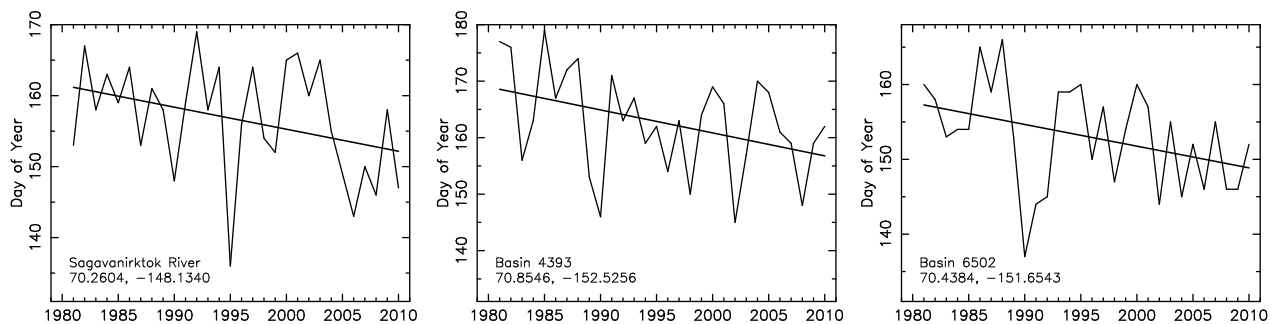


Figure S9: Date of maximum daily Q over period 1981–2010 for the three North Slope rivers with a significant ($p < 0.05$) trend to earlier maximum daily Q. The Sagavanirktok is the largest of the three. Linear least squares fit, basin name, and latitude and longitude coordinates shown.

Table S1: River basins ordered by size for the North Slope drainage region. Basins in the simulated topological network (STN) were defined on the 25×25 km² EASE-Grid (Brodzik and Knowles, 2002). Areas in km² based on extent in the STN of the full drainage basin expressed to the respective river mouth at the coast. Names listed for rivers with areas greater than 4000 km². Unnamed rivers are numbered by size among all river basins in the pan-Arctic STN.

Latitude	Longitude	Basin area	Name
70.3288	-151.0736	64095	Colville
70.6501	-154.3348	18851	Ikpikpuk
70.2604	-148.1340	16338	Sagavanirktok
70.9372	-156.1757	12568	Meade
70.3802	-148.6959	10054	Kuparuk
69.4239	-139.4672	6284	Firth
70.0799	-146.1292	5655	Canning
69.8753	-144.1624	5027	Hulahula
70.0150	-147.0306	4399	Shaviovik
68.5119	-135.8551	4399	Unnamed
70.8438	-155.5560	3770	Basin 1659
69.5061	-141.7360	3142	Basin 1882
68.6613	-137.1530	3142	Basin 1896
69.9243	-143.2594	2514	Basin 1949
69.7866	-142.7447	2514	Basin 1966
69.1231	-138.5215	2514	Basin 2012
68.6711	-136.2922	2514	Basin 2041
69.6471	-142.2369	2514	Basin 2104
68.8289	-136.7357	1885	Basin 2279
68.9706	-138.0587	1885	Basin 2354
70.1386	-147.5789	1885	Basin 2463
69.5720	-139.9503	1885	Basin 2464
68.6760	-135.4308	1885	Basin 2466
71.2383	-156.5290	1257	Basin 3496
70.9549	-154.6538	1257	Basin 3497
70.3011	-149.6013	1257	Basin 3498
69.9515	-145.5915	1257	Basin 3500
69.8212	-145.0607	1257	Basin 3501
69.2742	-138.9909	1257	Basin 3503
69.3244	-135.4441	1257	Basin 3504
70.8546	-152.5256	628	Basin 4393
70.4159	-150.1729	628	Basin 4394
69.5415	-140.8446	628	Basin 4398
69.0003	-135.4374	628	Basin 4409
68.8388	-135.0000	628	Basin 4410
69.3244	-134.5559	628	Basin 4416
69.4845	-134.1048	628	Basin 4419
71.1461	-155.8978	628	Basin 6501
70.4384	-151.6543	628	Basin 6502
70.0604	-143.7812	628	Basin 6507
68.8167	-137.6026	628	Basin 6511
69.1605	-135.8814	628	Basin 6513